Sensors and Actuators B xxx (2016) xxx–xxx

Contents lists available at ScienceDirect

Sensors and Actuators B: Chemical

journal homepage: www.elsevier.com/locate/snb

Polypyrrole/TiO_2 composites for the application of photocatalysis

Habib Ullah*, Asif Ali Tahir*, Tapas K. Mallick

Environment and Sustainability Institute (ESI), University of Exeter, Penryn Campus, Penryn, Cornwall TR10 9FE, UK

ARTICLE INFO

Article history:
Received 17 March 2016
Received in revised form 4 October 2016
Accepted 5 October 2016
Available online xxx

Keywords:
Band gap engineering
DFT
Molecular interaction
Photocatalysis
Redox potential

ABSTRACT

Density functional theory (DFT) study of polypyrrole-TiO_2 composites has been carried out to explore their optical, electronic and charge transfer properties for the development of an efficient photocatalyst. Titanium dioxide ($Ti_{16}O_{32}$) was interacted with a range of pyrrole (Py) oligomers to predict the optimum composition of nPy-TiO_2 composite with suitable band structure for efficient photocatalytic properties. The study has revealed that Py-$Ti_{16}O_{32}$ composites have narrow band gap and better visible light absorption capability compared to individual constituents. The simulated results of band structure (band gap, and band edge positions), molecular orbitals, and UV–vis spectra of the optimized nPy-$Ti_{16}O_{32}$ systems strongly support the existence of strong interactions between Py and TiO_2 in the composite. A red-shifting in λ_{max}, narrowing band gap, and strong intermolecular interaction energy (-41 to −72 kcal/mol) of nPy-$Ti_{16}O_{32}$ composites confirm the existence of strong covalent type interactions. Electron–hole transferring phenomena are simulated with natural bonding orbital analysis where Py oligomers found as donor and $Ti_{16}O_{32}$ as an acceptor in nPy-$Ti_{16}O_{32}$ composites.

1. Introduction

Nanostructured TiO_2 is one of the most investigated photoactive materials due to its excellent electronic structure and high stability to photocorrosion under redox conditions [1–3]. TiO_2 has drawn much attention due to its potential applications in solar energy conversion (such as photocatalytic water splitting and dye-sensitized solar cell), environmental cleaning (photocatalytic degradation of pollutants, self-cleaning, and water purification), and bio-sensing [4–7]. The solar energy conversion and photocatalytic efficiency of TiO_2 is limited due to its wide band gap (3.20 eV), as it can only absorb UV region of the solar spectrum [8]. Along with wide band gap, TiO_2 also suffer from high charge recombination rate (photogenerated electron–hole pair) which hindered the photocatalytic activity [9]. Strategies such as noble metal deposition as co-catalyst, metal or non-metal doping and photosensitization have been adopted to tailor band gap and enhance the charge transport properties to improve the photocatalytic performance of TiO_2 [10,11].

Conjugated organic polymer (COPs) [12–14] having spatially extended π-bonding system become potential energy materials due to their unique electrical and optical properties, such as high photon absorption coefficients under visible light irradiation, high electron mobility, excellent stability, material diversity, mechanical flexibility, light weight, low-temperature processing, roll to roll printing and large-area capability [15]. They have been successfully applied in organic electronic devices and solar cells [16]. Conducting polymers are mostly *p*-type semiconductors which work as an electron donor in the *p*-*n* junction solar cell. Polyaniline (PANI), polypyrrole (PPy), polythiophene (PT), polyacetylene (PA), polythiopene (PT), polyparaphenylene (PPP), polyparaphenylenevenylene (PPV), poly (3,4-ethylenedioxythiophene) (PEDOT), poly(*o*-phenylenediamine) (POPD) are prominent examples of COPs which are being explored in this area [12–14,17]. Recently, it has been found that composite of metal oxide and COP into intimate contact on both physical and electronic levels have significantly improved solar energy conversion and photocatalytic performance compared to metal oxide or COP individually [18]. Moreover, an increasing interest is found on the fabrication of COP-TiO_2 nanocomposites for photocatalytic degradation of environmental pollutants as well as water splitting to generate hydrogen [19,20].

Although, experimental study of PPy-TiO_2 as a photocatalyst is reported but facing lower photocatalytic efficiency which is due to lack of theoretical investigation [21–24]. The fully explored theoretical insight of optical, electronic structure, surface interactions, electroactivity and charge transfer mechanism between PPy and TiO_2 is essential to tailor and improve photocatalytic activity of PPy-TiO_2 nanocomposite. Our recent investigation on PPy and pyrrole oligomers (nPy, where n is a number of repeating units) has proved

* Corresponding authors.
E-mail addresses: Hu203@exeter.ac.uk (H. Ullah), A.Tahir@exeter.ac.uk (A.A. Tahir).

http://dx.doi.org/10.1016/j.snb.2016.10.019
0925-4005/

that nPy has excellent tunable, optical and electroactive properties [25–27]. In this work, we have detailed theoretical investigation of charge transfer mechanism between nPy and TiO_2 (molecular cluster; $Ti_{16}O_{32}$) in a connected junction such as nPy-TiO_2 nanocomposite. The present article is focused on the investigation of important photocatalytic parameters such as (i) interaction of $Ti_{16}O_{32}$ with PPy oligomers to find out electron–hole transformation, (ii) band structure alteration, (iii) mechanism of charge (electron/hole) transport (vi) optimisation of oligomeric length of Py for efficient performance and (v) structure-property relationship. The study is aimed to provide a better understanding of the electronic structure of nPy-$Ti_{16}O_{32}$ nanocomposite and will open new direction to synthesize an efficient nPy-TiO_2 nanocomposite photocatalyst with the optimized composition for visible light photocatalysis. Moreover, this work will also inspire computational scientists to explore structural property relationship of other COP-metal oxide nanocomposites.

2. Methodology

Interaction of molecular cluster of $Ti_{16}O_{32}$ with nPy oligomers (n = 3, 5, and 9) are performed with the help of density functional theory (DFT). All DFT calculations [28,29] were carried out on *GAUSSIAN 09* [30] and the results were visualized through *Gabedit* [31], *GaussSum* [32], and *GaussView* [33]. DFT and time-dependent DFT (TD-DFT) calculations were performed at B3LYP with LanL2DZ basis set for the determination of electronic structure properties of nPy-$Ti_{16}O_{32}$, as an efficient photocatalyst. Oligomers up to eight repeating units can accurately represent its polymeric characteristics so, oligomeric size is restricted to nine repeating units [28,29]. A molecular cluster of $Ti_{16}O_{32}$ is added to the oligomeric backbone of nPy and then optimized. Geometries of nPy-$Ti_{16}O_{32}$ (n = 3 to 9) systems were optimized at B3LYP/LanL2DZ level and confirmed from frequency calculations. The non-bonding and bonding interaction energies in nPy-$Ti_{16}O_{32}$ are simulated with help of interaction energy (ΔE_{Int}) and geometrical counterpoise correction (gCP). The gCP is able to treat both inter- and intra-molecular BSSE on the same footing at low computational cost. The B3LYP-gCP-D3 [34] interaction energy is simulated from the Grimme Web service [35]. The ΔE_{Int} and gCP-D3 are calculated from equations 1 and 2, respectively.

$$\Delta E_{int} = E_{Ti16O32} + E_{nPy} - E_{nPy-Ti16O32} \quad (1)$$

$$\Delta E_{gCP-D3} = E_{(nPy-Ti16O32)gCP-D3} - E_{(nPy)gCP-D3} - E_{(Ti16O32)gCP-D3} \quad (2)$$

UV–vis spectra are simulated at hybrid TD-DFT with pseudopotential of LanL2DZ. Natural bonding orbitals (NBO) analysis performed for the charge simulations. All these calculations were performed in the gas phase.

Table 1
Electronic properties of isolated TiO_2, $Ti_{16}O_{32,and}$ $Ti_{28}O_{56}$ Anatase clusters.

Species	Band gap (eV)	HOMO (eV)	LUMO (eV)	Optical gap (nm)
$Ti_{16}O_{32}$	3.06	−7.33	−4.33	333
$Ti_{28}O_{56}$	2.61	−7.39	−4.78	471
Isolated TiO_2	1.86	−5.28	−3.42	647

3. Results and discussion

3.1. Choice of TiO_2 cluster

To understand physical significance of nPy-TiO_2 at the molecular level, it is important to select an appropriate TiO_2 cluster as a representative of its bulk. The interactions between nPy and TiO_2 surface can be described in two different ways; the cluster model and periodic surface models [36]. For the surface representation of TiO_2, we have used cluster models, consisting of 48 and 84 atoms which are applicable to the molecular quantum chemistry [36]. Electronic properties such as HOMO, LUMO, band gap, and optical gap of isolated TiO_2, $Ti_{16}O_{32}$, and $Ti_{28}O_{56}$ clusters are simulated which are comparatively listed in Table 1. On the basis of band gap simulation and computational point of view, it is evident that $Ti_{16}O_{32}$ (band gap 3.06 eV) is a better representative of bulk anatase (Fig. 1). The current study is focused on $Ti_{16}O_{32}$ and their interaction with different Py oligomers.

3.2. Optimized geometries

Geometrical relaxation of nPy, $Ti_{16}O_{32,}$ and nPy-$Ti_{16}O_{32}$ bound species are carried out at DFT- B3LYP/LanL2DZ level. Optimized geometric structure of 48 atoms ($Ti_{16}O_{32}$) is given in Fig. 1, while their comparative geometrical parameters are listed in Table 2. Analysis of the data (Table 2) proves that there is no significant difference between geometrical parameters of bulk (crystal/condensed phase) and molecular cluster (gas phase), confirming that $Ti_{16}O_{32}$ is the best representative of bulk TiO_2.

The optimized geometric structures of 7Py-$Ti_{16}O_{32}$ and 9Py-$Ti_{16}O_{32}$ along with their inter-molecular bond distances are shown in Figs. 2 and 3, respectively, while 3Py-$Ti_{16}O_{32}$ and 5Py-$Ti_{16}O_{32}$ are given in S1 and S2 of the Supplementary information. During the optimization, $Ti_{16}O_{32}$ circulated and finally attached at the middle of nPy oligomer by establishing strong non-covalent bonds with H and C atoms of Py. The interaction of $Ti_{16}O_{32}$ with nPy oligomers, results distortion in nPy geometries (Figs. 2 and 3), which is a direct consequence of their strong orbital overlapping. Six different types of inter-molecular interactions are observed in the case of the 7Py-$Ti_{16}O_{32}$ system; where Ti and O of $Ti_{16}O_{32}$ have made the strong electrostatic type of bonding with the C and H atoms of 7Py; ranging at ca. 1.90 to 2.80 Å. In all these composites, Ti atom of $Ti_{16}O_{32}$

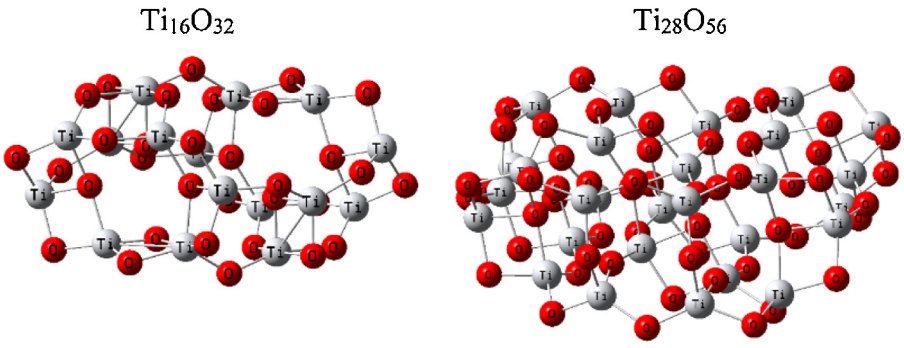

Fig. 1. Optimized Geometric Structure of $Ti_{16}O_{32}$ and $Ti_{28}O_{56}$ clusters.

Please cite this article in press as: H. Ullah, et al., Polypyrrole/TiO_2 composites for the application of photocatalysis, Sens. Actuators B: Chem. (2016), http://dx.doi.org/10.1016/j.snb.2016.10.019

Table 2
B3LYP/LanL2DZ ground states bond angles and distances in the Vacuum for Molecular TiO_2, cluster of $Ti_{16}O_{32}$, and in the Bulk for structural Rutile and Anatase.

Parameters	This study	TiO_2 Vacuum	TiO_2 Vacuum[1]	Rutile bulk properties[1]	Anatase bulk properties[1]
dTi–O	1.71/92 Å	1.63 Å	1.67 Å	1.96 Å	1.83 Å
dTi–Ti	2.78 Å	–	–	3.61 Å	3.03 Å
dO–O	2.46 Å	–	–	2.57 Å	2.29 Å
O–Ti–O	82.96°	110.7°	110.6°	81.6°	74.1°
Ti–O–Ti	102.82°	–	–	130.8°	105.9°

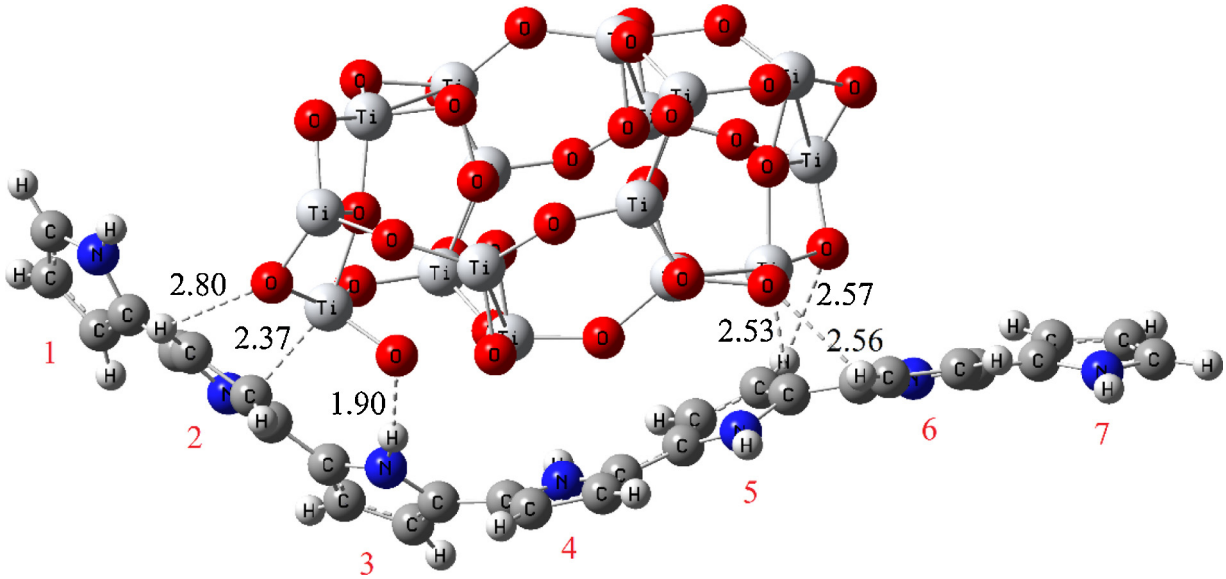

Fig. 2. Optimized Geometric Structure of 7Py-$Ti_{16}O_{32}$.

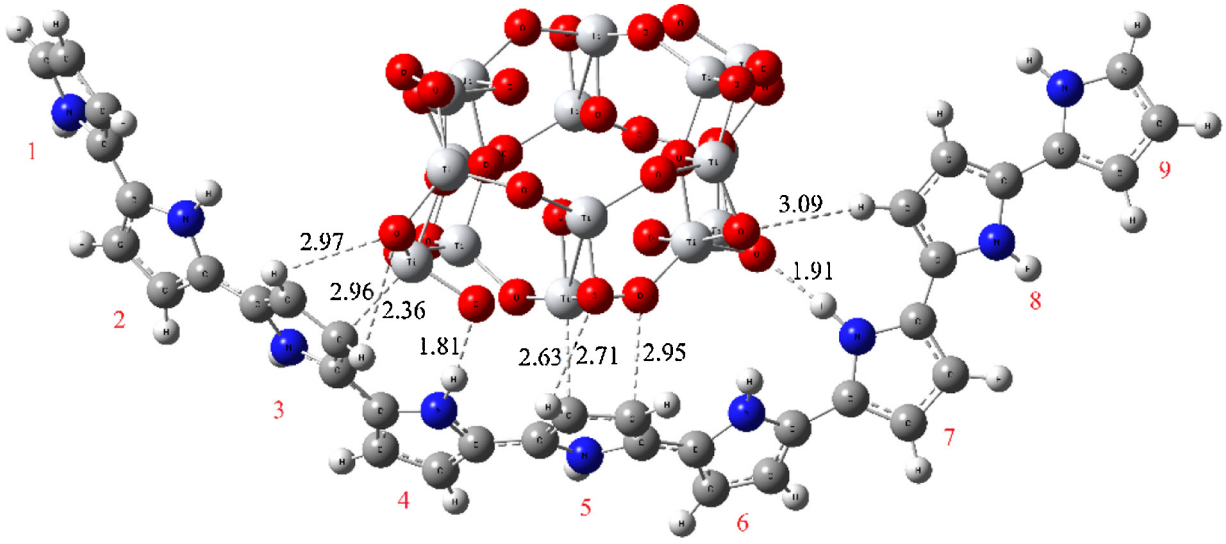

Fig. 3. Optimized Geometric Structure of 9Py-$Ti_{16}O_{32}$.

makes an inter-molecular electrostatic bond with C of nPy and a Hydrogen bond between the O of $Ti_{16}O_{32}$ and H atoms of nPy.

The O—H inter-molecular bonds in the studied systems are strong bonds and can be regarded as covalent bonding. On the other hand, simulated Ti—C bond distances in the range of 2.30–2.70 Å confirm the formation of a strong electrostatic interaction. Jeffery et al. have reported that 2.2–2.5 Å of hydrogen bonding will be "strong, mostly covalent", 2.5–3.2 Å as "moderate, mostly electrostatic" while 3.2–4.0 Å as "weak, mostly electrostatic" along with following bond energies, −40 to −14, −15 to −4, and <−4 kcal/mol, respectively [37]. Comparative analysis of simulated inter-molecular bonding (including Fig. S1 and S2) led us to conclude that $Ti_{16}O_{32}$ make a strong composite with Py oligomers.

3.3. *Interaction energy in nPy-$Ti_{16}O_{32}$ composites*

$Ti_{16}O_{32}$ and PPy oligomers have a good interaction which is mostly covalent and electrostatic, simulated from interaction energy (ΔE_{int}) and geometrical counterpoise corrected ($\Delta E_{gCP\text{-}D3}$) methods (Table 3). The $\Delta E_{gCP\text{-}D3}$ method is employed to minimize the geometrical and dispersion factors. The result of this

Please cite this article in press as: H. Ullah, et al., Polypyrrole/TiO_2 composites for the application of photocatalysis, Sens. Actuators B: Chem. (2016), http://dx.doi.org/10.1016/j.snb.2016.10.019

Table 3
Inter-molecular interaction energy (ΔE_{int}), geometrical counterpoise corrected energy (ΔEgCP-D3), in kcal/mol), and NBO charges analysis of nPy-$Ti_{16}O_{32}$.

Species	ΔE_{int}	ΔE_{gCP-D3}	Q_{NBO}
3Py-$Ti_{16}O_{32}$	−42.54	−54.09	0.409
5Py-$Ti_{16}O_{32}$	−34.22	−47.50	0.469
7Py-$Ti_{16}O_{32}$	−41.10	−72.47	0.709
9Py-$Ti_{16}O_{32}$	−41.47	−68.21	0.599

inter-molecular interaction energy proved that a very strong interaction is present in nPy and $Ti_{16}O_{32}$ species. In the 3Py-$Ti_{16}O_{32}$ composite, the ΔE_{int} is −42.54 kcal/mol while this interaction energy is simulated to be −54.09 kcal/mol with ΔE_{gCP-D3} method which is 11.55 kcal/mol higher than the ΔE_{int} method.

A comparatively weak inter-molecular forces are present in 5Py-$Ti_{16}O_{32}$ for which these energies are; −34.22 kcal/mol based on ΔE_{int} and −47.50 kcal/mol based on ΔE_{gCP-D3}. This decrement in inter-molecular interaction energy is due to its geometrical shape compared to the 3Py-$Ti_{16}O_{32}$ composite. With chain length elongation, a slight difference in ΔE_{int} is observed as can be seen from data in Table 3. In the case of 7Py-$Ti_{16}O_{32}$, this inter-molecular non-bonding energy is about −41.10 kcal/mol, based on ΔE_{int} while −72.47 kcal/mol based on ΔE_{gCP-D3}. This highest interaction energy (ΔE_{gCP-D3}) in 7Py-$Ti_{16}O_{32}$ can be attributed to the suitable oligomeric length of PPy. Moreover, strong interaction of 7Py-$Ti_{16}O_{32}$ can be correlated to the fully relaxed geometric structure, which allows 7Py to wrap around $Ti_{16}O_{32}$ cluster much effectively compared to other compositions of nPy-$Ti_{16}O_{32}$ (Fig. 2). A similar but less pronounced trend is observed in 9Py-$Ti_{16}O_{32}$ composite, where the ΔE_{int} and ΔE_{gCP-D3} are −41.47 and −68.21 kcal/mol, respectively. Comparative analysis of the interaction energy of 7Py-$Ti_{16}O_{32}$ and 9Py-$Ti_{16}O_{32}$ indicate that 7Py make stronger nanocomposite. In summary, the amount of this interaction energy also evidences the existence of strong types of bonds between these two species which led to the confirmation of stable composite.

3.4. Natural bonding orbital analysis

Inter-molecular charge transfer between nPy and $Ti_{16}O_{32}$ are simulated with natural bonding orbital (Q_{NBO}) charge analysis at B3LYP with pseudopotential of LanL2DZ. As discussed elsewhere, these charge analyses are basis set dependent but with the same level of theory [such as B3LYP/6-31G (d), UB3LYP/6-31G (d), UB3LYP/6-311++G (d, p) or B3LYP/LanL2DZ] etc., for different structures the results would provide meaningful trends [38,39].

In connection with previous sections, $Ti_{16}O_{32}$ interacts with nPy oligomers through strong hydrogen (mostly covalent) and electrostatic (Ti—C). The analysis of NBO simulation indicates that Ti—C bond is the main charge transferring paths in all nPy-$Ti_{16}O_{32}$ composites. The net charge transfer in all nPy-$Ti_{16}O_{32}$ composites is listed in Table 3 while individual ring charges are listed in Table 4 along with $Ti_{16}O_{32}$ attached-Py rings. Analysis of data in Table 4 confirms the electron accepting nature of $Ti_{16}O_{32}$ in the composite as it withdraws electronic cloud density from Py oligomers to about 0.40 to 0.70 e^- which results in a cationic state in nPy oligomers, responsible for better electrical conductivity [40–42].

Table 5
Molecular Orbital Energy, Band Gap (in eV) and Dipole moment (Debye) of nPy and nPy- $Ti_{16}O_{32}$ composites.

Species	HOMO	LUMO	Dipole moment	Band Gap
$Ti_{16}O_{32}$	−7.33	−4.27	0.0007	3.06
3Py	**−4.71**	**−0.44**	**1.56**	**4.27**
3Py-$Ti_{16}O_{32}$	−5.67	−2.12	13.63	2.55
5Py	**−4.45**	**−0.76**	**1.08**	**3.69**
5Py-$Ti_{16}O_{32}$	−5.04	−3.53	10.89	1.51
7Py	**−4.34**	**−0.91**	**0.58**	**3.43**
7Py-$Ti_{16}O_{32}$	−5.24	−3.37	9.97	1.87
9Py	**−4.28**	**−0.98**	**0.07**	**3.30**
9Py-$Ti_{16}O_{32}$	−4.42	−3.68	8.75	0.74

Finally, a unique charge distribution can be seen in the Py rings of 7Py-$Ti_{16}O_{32}$ system which suggest that 7Py-$Ti_{16}O_{32}$ is an optimum composition with greater charge transferring ability.

3.5. Electronic properties simulation

The electronic properties such as IP, EA, HOMO, LUMO, ESP, DOS and band gap of isolated as well as nPy-$Ti_{16}O_{32}$ composites was estimated at B3LYP/LanL2DZ level. The ΔSCF and negative of HOMO orbital energies are almost similar, especially for long chain systems. The IP energy is estimated from the negative of HOMO while the EA is obtained from negative of LUMO, using Koopman's theorem. Higher the EA and IP values of a chemical substance, greater will be its electroactivity and stability. The HOMO and LUMO energies (band edge positions) of isolated $Ti_{16}O_{32}$ are listed in Table 5 while frontier molecular orbitals are shown in Fig. 4.

Our simulated band gap value for $Ti_{16}O_{32}$ is 3.06 eV at B3LYP/LanL2DZ level, which is close to that of the observed data (3.20 eV) [40]. The difference is because of molecular cluster simulation as reported by Troisi et al. [41]; different simulation packages, cluster size, and level of theories give rise to different band gaps. Usually, the band gap decrease with increase in the size of the cluster and it is expected that this will also converge to the bulk value like that of the total energy [41]. Best reactive sites of both of the $Ti_{16}O_{32}$ and nPy oligomers are estimated from molecular electrostatic potential (MEP) as shown in Fig. 4 and 5. Based on these MEP plots, $Ti_{16}O_{32}$ and nPy oligomers interacted at a suitable distance.

3.6. Ionization potential

Interaction of $Ti_{16}O_{32}$ with nPy increases the IP of nPy oligomers indicating the increased stability of the resulted composite as can be seen from the delocalized contours (Fig. 5). Higher the IP more will be the stability of a chemical substance. In case of 3Py-$Ti_{16}O_{32}$ composite, the increase in IP is about 0.96 eV which consequently narrow its band gap from 4.27 to 2.12 eV (as discussed in band gap section below). A similar trend is observed in rest of the nPy oligomers in nPy-$Ti_{16}O_3$ composites, except 9Py-$Ti_{16}O_3$ composite, where negligible change (IP value) has been observed which can be attributed to lower interaction ability of their molecular orbitals. The increase in IP value of nPy-$Ti_{16}O_3$ composites is clearly depicted in Fig. 6.

Table 4
NBO charge Analysis in unit of electron of nPy-$Ti_{16}O_{32}$ rings.

Species	Ring 1	Ring 2	Ring 3	Ring 4	Ring 5	Ring 6	Ring 7	Ring 8	Ring 9
3Py-$Ti_{16}O_{32}$	0.228	0.11	0.071						
5Py-$Ti_{16}O_{32}$	0.087	0.102	0.204	0.034	0.042				
7Py-$Ti_{16}O_{32}$	0.065	0.16	0.103	0.108	0.121	0.105	0.047		
9Py-$Ti_{16}O_{32}$	0.039	0.043	0.158	0.126	0.156	0.041	0.021	0.011	0.004

Please cite this article in press as: H. Ullah, et al., Polypyrrole/TiO_2 composites for the application of photocatalysis, Sens. Actuators B: Chem. (2016), http://dx.doi.org/10.1016/j.snb.2016.10.019

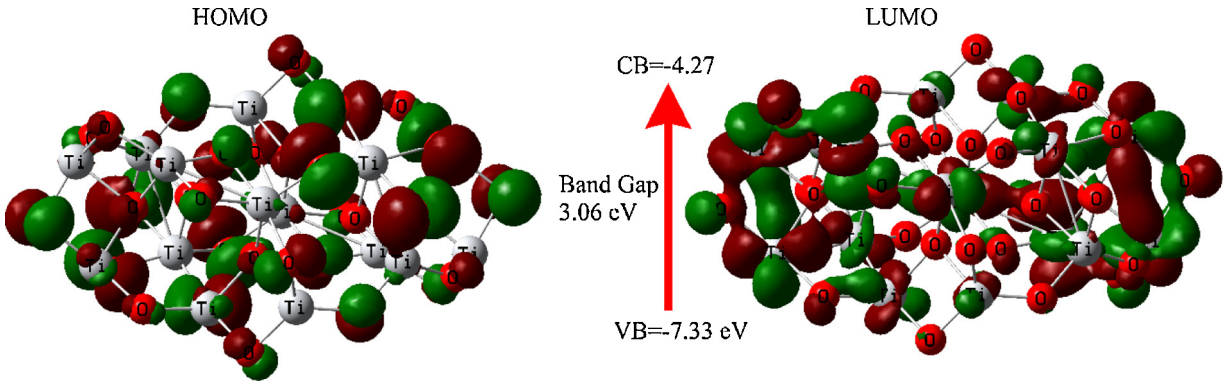

Fig. 4. Contours of the HOMO and LUMO of $Ti_{16}O_{32}$.

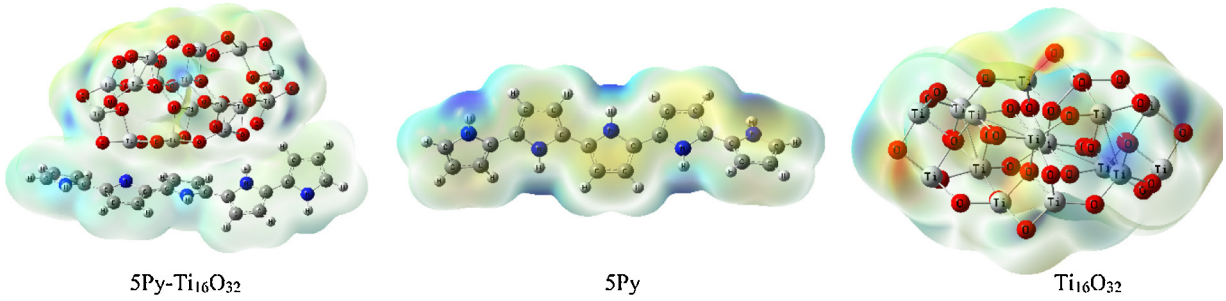

Fig. 5. Molecular Electrostatic Potential plots of $Ti_{16}O_{32}$, 5Py and 5Py-$Ti_{16}O_{32}$.

3.6.1. Electron affinitie

EA is estimated from the negative of LUMO, which found to be increasing in nPy oligomers upon interacting with $Ti_{16}O_{32}$. A substantial shift in LUMO to narrow the band gap is observed in nPy-$Ti_{16}O_{32}$ bounded species compared to individual $Ti_{16}O_{32}$ and nPy as shown in Fig. 7. $Ti_{16}O_{32}$ shifts the EA of 3Py from 0.44 to 2.12 eV, 2.77 eV in 5Py-$Ti_{16}O_{32}$, 2.46 eV in 7Py-$Ti_{16}O_{32}$ and 2.70 eV in 9Py-$Ti_{16}O_{32}$ composite. As discussed in the optimized geometric analysis, $Ti_{16}O_{32}$ has an excellent interaction with nPy oligomers which is also in agreement with the EA analysis. The overall increase in EA value proves that the nPy-$Ti_{16}O_{32}$ composites are cationic in nature where polaron and bipolaron states may exist.

3.6.2. Band gap and molecular orbitals energy

Both optical and electrical band gaps are simulated at ΔSCF (excitation energy with higher oscillator strength) and B3LYP (difference of HOMO-LUMO orbitals), listed in Tables 5 and 6 . Analysis of the data (Table 5) clarifies that the band gap of nPy oligomers become narrow upon interaction with $Ti_{16}O_{32}$, which is an evidence of their excellent electroactive property in the resulted composite.

Frontier molecular orbitals and dipole moments of these interacting species before and after interaction are calculated at B3LYP/LanL2DZ level. The contours of HOMO and LUMO along with band gap of nPy and nPy-$Ti_{16}O_{32}$ composites are given in Figs. 8 and 9, respectively. It can be easily predicted from the date that molecular orbitals of $Ti_{16}O_{32}$ strongly interact with the

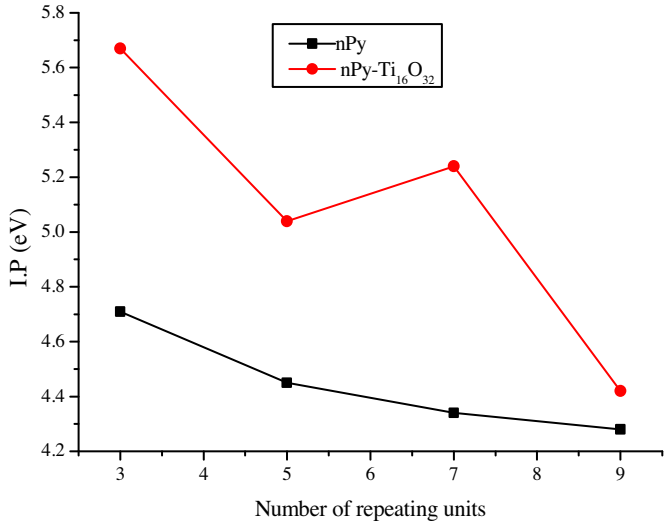

Fig. 6. Change in IP of nPy and nPy-$Ti_{16}O_{32}$ composites.

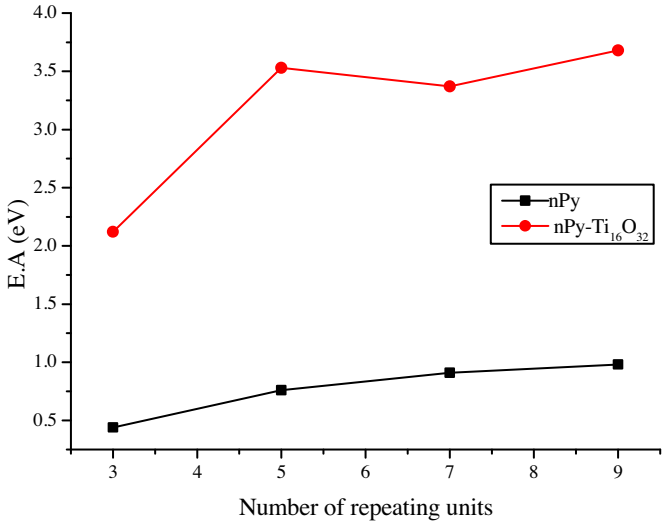

Fig. 7. Change in E.A of nPy and nPy-$Ti_{16}O_{32}$ composites.

Please cite this article in press as: H. Ullah, et al., Polypyrrole/TiO_2 composites for the application of photocatalysis, Sens. Actuators B: Chem. (2016), http://dx.doi.org/10.1016/j.snb.2016.10.019

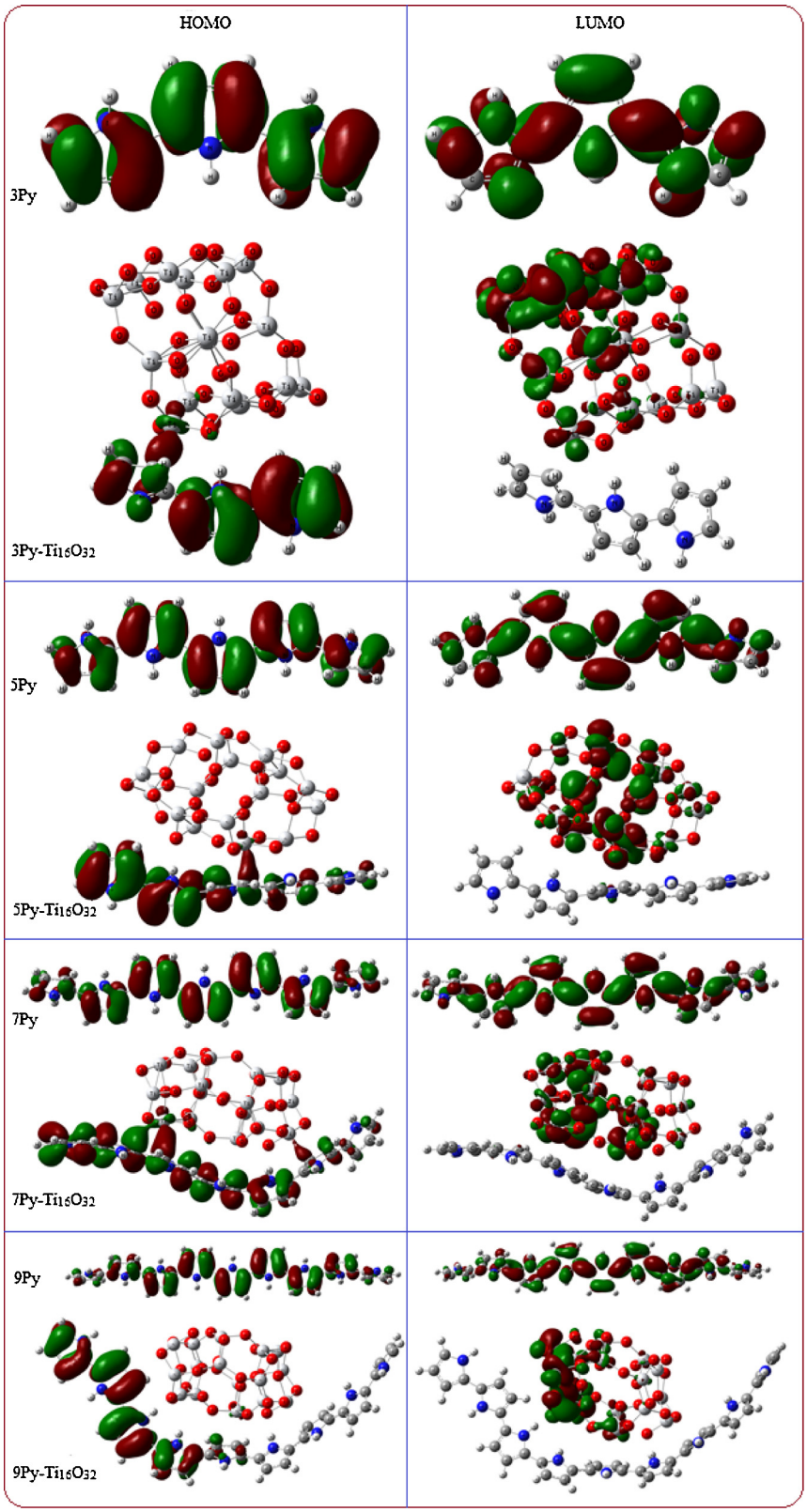

Fig. 8. Frontier molecular orbitals of $Ti_{16}O_{32}$, nPy and nPy-$Ti_{16}O_{32}$ bounded complexes.

HOMO/LUMO of nPy through establishing strong covalent types of bonding (Table 5). The strong covalent type of bonding indicate the stability of nPy-$Ti_{16}O_{32}$ composites which have an intermediate band gap and highest dipole moment.

The LUMO energy of $Ti_{16}O_{32}$ has considerably reduced from −0.44 to −2.12 eV while the band gap of Py reduced from 4.27 to 2.55 eV in all nPy-$Ti_{16}O_{32}$ composites as shown in Figs. 8 and 9. Dipole moment of 3Py-$Ti_{16}O_{32}$ (13.63 Debye) clearly demonstrates a substantial increment in its electroactivity.

Please cite this article in press as: H. Ullah, et al., Polypyrrole/TiO_2 composites for the application of photocatalysis, Sens. Actuators B: Chem. (2016), http://dx.doi.org/10.1016/j.snb.2016.10.019

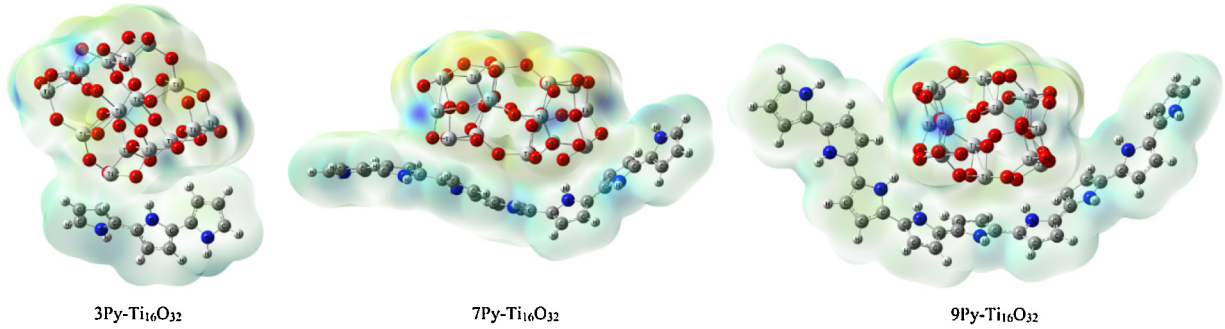

Fig. 9. Molecular electrostatic potential plot of 3, 7 and 9Py-$Ti_{16}O_{32}$ composites.

Moreover, narrowing band gap, have also a direct relationship with chain length elongation of Py as obvious from Fig. 10. $Ti_{16}O_{32}$ reduces the HOMO of 5Py from −4.45 to −5.04 eV (actually increase in negative charge), LUMO from −0.76 to −3.53 eV and band gap from 3.69 to 1.51 eV. Similar, but more pronounced reduction in these values can be seen in 7Py-$Ti_{16}O_{32}$, 0.90 eV in HOMO, 2.46 eV in LUMO, and a reduction of 1.56 eV in its band gap. Electronic cloud densities of the contours of HOMO and LUMO of 9Py-$Ti_{16}O_{32}$ compared to that of 9Py are enhanced to about 0.14 eV and 2.70 eV, respectively. While their dipole moment and band gap change from 0.07 to 8.75 Debye and 3.30 to 0.74 eV, respectively. The molecular electrostatic potential plot of 3, 7 and 9Py-$Ti_{16}O_{32}$ are shown in Fig. 9, which clearly visualize their electroactive nature. Furthermore, the density of states plots for four these composites are correlatively shown in Fig. 10, which highlight a substantial variation in their band edges shifting compared to their individual constituents.

The homogeneous MEP plot (Fig. 9) of these composites confirm the excellent interaction between nPy and $Ti_{16}O_{32}$ cluster by mutually sharing of their electronic cloud densities. One can easily observe how the HOMO and LUMO of $Ti_{16}O_{32}$ (red spectra) and nPy (black spectra) interacted and resulted stable and ideal (align band edges with redox potential of water) nPy-$Ti_{16}O_{32}$ (blue spectra) composites. This theoretical investigation will guide and minimize the synthetic effort in term of interaction and mixing ratios. So, from experimental point view, we don't need to synthesize an

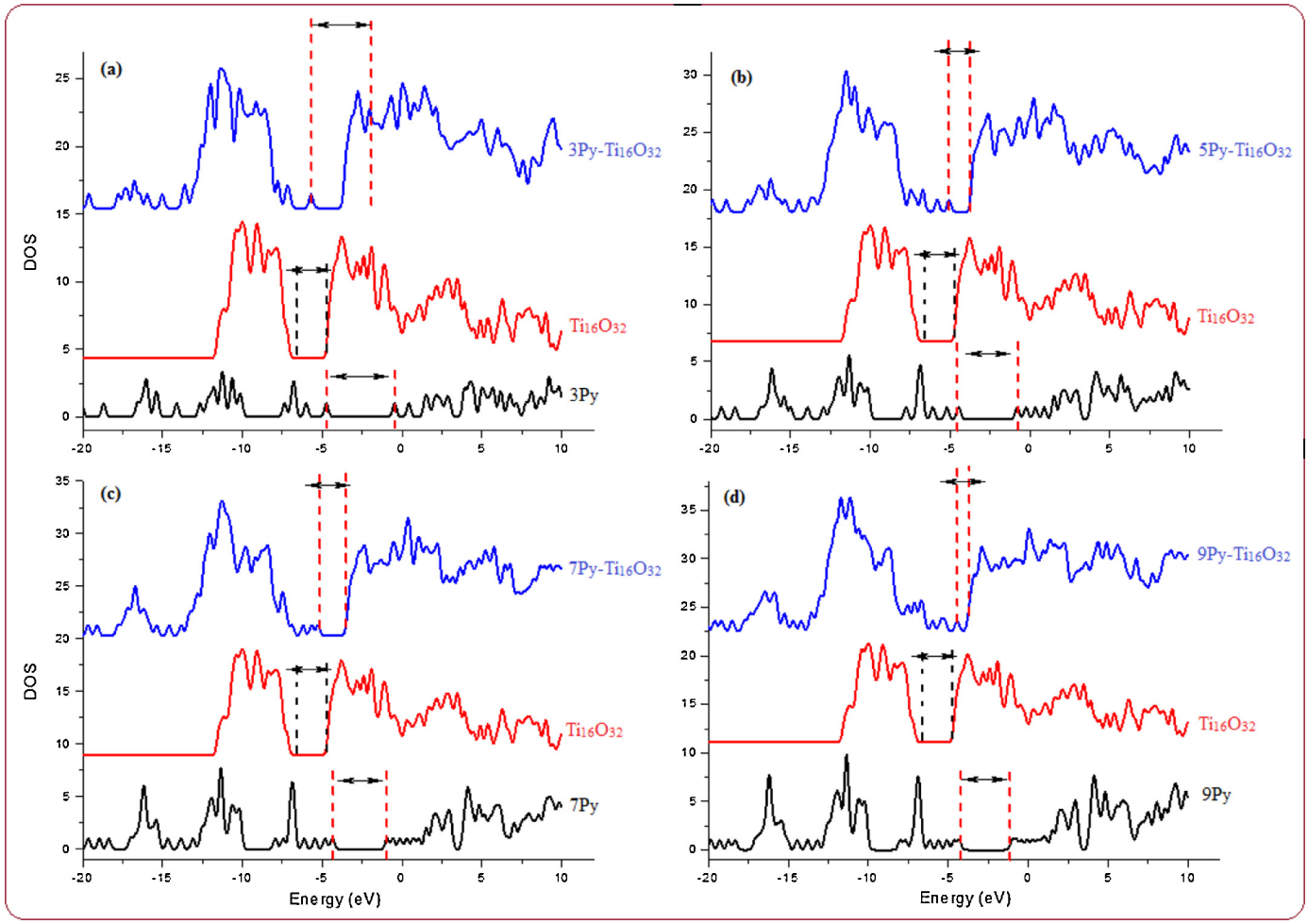

Fig. 10. Density of states plots of $Ti_{16}O_{32}$, nPy and nPy-$Ti_{16}O_{32}$ bounded complexes.

Please cite this article in press as: H. Ullah, et al., Polypyrrole/TiO_2 composites for the application of photocatalysis, Sens. Actuators B: Chem. (2016), http://dx.doi.org/10.1016/j.snb.2016.10.019

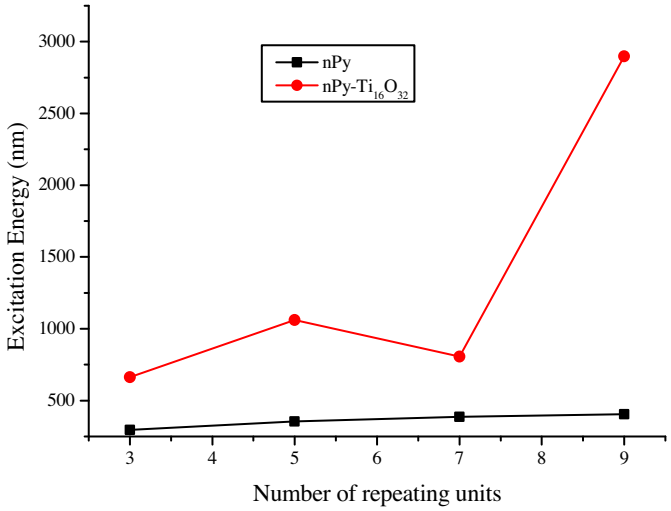

Fig. 11. First allowed electronic excitation energy of nPy and nPy-$Ti_{16}O_{32}$ composites.

infinite chain length of PPy, the routine oligomer (up to 6 or 8 repeating units) will be a best fit for the commercially available TiO_2 (anatase). Furthermore, the study also provides insight into improving the band structure, charge transport and determination of physical and chemical bonding between nPy and TiO_2 species.

3.7. UV–vis study

UV–vis spectra of nPy, $Ti_{16}O_{32}$, and nPy- $Ti_{16}O_{32}$ are simulated in the gas phase at TD-DFT/UB3LYP/LanL2DZ level. The first allowed electronic excitation energies are correlated with the experimentally observed λ_{max}, which are listed in Fig. 11 and Table 6. Three prominent band peaks are found in the UV–vis spectra of nPy oligomers where the high wavelengths one is referred as λ_{max}; the transition of an electron from valence to conduction band. Interaction of $Ti_{16}O_{32}$ with nPy oligomers (Fig. 11 and Table 6) cause a red-shifting in the λ_{max} of nPy. This red-shifting in λ_{max} of all nPy oligomers illustrates the *n*-type doping nature of $Ti_{16}O_{32}$.

In the case of 3Py, the excitation energy of $\pi \rightarrow \pi^*$ transition increased from 296 to 663 nm in the resulted composite (3Py-$Ti_{16}O_{32}$), which evidences the establishment of strong bonding. As shown in Table 6, $Ti_{16}O_{32}$ increases the first allowed electronic excitation energy of 5Py to about 707 nm, 420 nm in 7Py, and 2493 nm in 9Py. This substantial increase can be attributed to improved conductivity/delocalization of the composites compared to isolated nPy oligomers (*vide infra*).

The individual $Ti_{16}O_{32}$ and nPy oligomers are unable to absorb in the visible range, however, nPy-$Ti_{16}O_{32}$ composites have excellent absorption capability in the visible region (Table 6) due to a substantial decrease in the band gap. The red-shifting from the ultraviolet to visible elucidates/evidences the excellent photovoltaic and photocatalytic activity of nPy-$Ti_{16}O_{32}$ composites over their individual constituents. Analysis of the simulation results led us to conclude that all nPy-$Ti_{16}O_{32}$composites have a wide range of visible light absorption capability. Among the long chain oligomeric systems, the first allowed excitation energy of ($\pi \rightarrow \pi^*$ transition) of 9Py-$Ti_{16}O_{32}$ is more prominent compared to other compositions (Fig. 11) indicating that eight or nine repeating unit of PPy would be an excellent oligomeric chain length to develop an efficient visible light active photocatalyst (composite). This argument is also in good agreement with the other parameters discussed above.

Table 6
Calculated excitation energies, oscillator strengths, and molecular orbitals (MOs) of the first allowed singlet transition involved in the excitation for nPy and nPy-$Ti_{16}O_{32}$ composites.

Species	Energy (eV)	Wavelength (nm)	Oscillator Strength	MOs	Coefficient
$Ti_{16}O_{32}$	3.71	333	0.01	$S_0 \rightarrow S_1$	0.46
3Py	4.18	296	0.87	$S_0 \rightarrow S_1$	0.70
3Py-$Ti_{16}O_{32}$	1.86	663	0.005	$S_0 \rightarrow S_1$	0.37
5Py	3.49	354	1.50	$S_0 \rightarrow S_1$	0.70
5Py-$Ti_{16}O_{32}$	1.16	1061	0.008	$S_0 \rightarrow S_1$	0.50
7Py	3.19	387	2.08	$S_0 \rightarrow S_1$	0.70
7Py-$Ti_{16}O_{32}$	1.53	807	0.02	$S_0 \rightarrow S_1$	0.68
9Py	3.05	405	2.67	$S_0 \rightarrow S_1$	0.69
9Py-$Ti_{16}O_{32}$	0.42	2898	0.0002	$S_0 \rightarrow S_1$	0.70

4. Conclusions

Density functional theory study (DFT) of pyrrole-$Ti_{16}O_{32}$ bounded systems are carried out to find their interaction to tailor the best composite for the photodegradation of environmental pollutants and solar water splitting. Inter-molecular interaction energy in nPy-$Ti_{16}O_{32}$ composites is simulated in the range of −41 to −72 kcal/mol which confirmed the existence of strong covalent and electrostatic type bonding. This energy is simulated with the help of single point energy and ΔEgCP-D3 methods. So, after confirming the composite formation, band gap narrowing and better visible light absorption capability is observed compared to their individual nPy and $Ti_{16}O_{32}$ constituents. Electronic properties such as HOMO and LUMO of nPy, $Ti_{16}O_{32}$ and nPy-$Ti_{16}O_{32}$ composites estimated using B3LYP/LanL2DZ level, indicate excellent visible light absorption and charge transport efficiency of nPy-$Ti_{16}O_{32}$. Other electronic properties such as ESP, DOS, band gap, and UV–vis spectra also support the formation of efficient photoactive nPy-$Ti_{16}O_{32}$ composites. Moreover, UV–vis spectra of these composites predict the visible light absorption compared to nPy and $Ti_{16}O_{32}$. Electron-hole transferring define Py oligomers as a donor and $Ti_{16}O_{32}$ cluster as an acceptor in the resulted composites. Finally, the oligomeric length of eight/nine in the composite is found to be an optimum for the designing of an efficient photocatalyst. This theoretical investigation will minimize the synthetic effort such as mixing ratios of TiO_2 and PPy oligomers. Although, other components present in the cell might affect the nPy-TiO_2 interactions, but this basic theoretical study guides us about its possibility to be used as a photocatalyst. The study will also guide experimental scientists to improve the band structure, optical, physical and chemical properties of COP-TiO_2 and other metal oxide composites.

Acknowledgment

H.U acknowledges the partial financial support of the UK Solar Fuel Network (SFN).

Appendix A. Supplementary data

Supplementary data associated with this article can be found, in the online version, at http://dx.doi.org/10.1016/j.snb.2016.10.019.

References

[1] S. Cherian, C.C. Wamser, Adsorption and photoactivity of tetra (4-carboxyphenyl) porphyrin (TCPP) on nanoparticulate TiO_2, J. Phys. Chem. B 104 (2000) 3624–3629.
[2] Y.-G. Kim, J. Walker, L.A. Samuelson, J. Kumar, Efficient light harvesting polymers for nanocrystalline TiO_2 photovoltaic cells, Nano Lett. 3 (2003) 523–525.
[3] I. Robel, V. Subramanian, M. Kuno, P.V. Kamat, Quantum dot solar cells Harvesting light energy with CdSe nanocrystals molecularly linked to mesoscopic TiO_2 films, J. Am. Chem. Soc. 128 (2006) 2385–2393.

[4] Y.-Y. Song, F. Schmidt-Stein, S. Bauer, P. Schmuki, Amphiphilic TiO_2 nanotube arrays: an actively controllable drug delivery system, J. Am. Chem. Soc. 131 (2009) 4230–4232.
[5] K. Woan, G. Pyrgiotakis, W. Sigmund, Photocatalytic carbon-nanotube–TiO_2 composites, Adv. Mater. 21 (2009) 2233–2239.
[6] V. Chabot, D. Higgins, A. Yu, X. Xiao, Z. Chen, J. Zhang, A review of graphene and graphene oxide sponge: material synthesis and applications to energy and the environment Energy, Environ. Sci. 7 (2014) 1564–1596.
[7] D. Wen, S. Guo, J. Zhai, L. Deng, W. Ren, S. Dong, Pt nanoparticles supported on TiO_2 colloidal spheres with nanoporous surface: preparation and use as an enhancing material for biosensing applications, J. Phys. Chem. C 113 (2009) 13023–13028.
[8] S. Banerjee, S.C. Pillai, P. Falaras, K.E. O'shea, J.A. Byrne, D.D. Dionysiou, New insights into the mechanism of visible light photocatalysis, J. Phys. Chem. Lett. 5 (2014) 2543–2554.
[9] N. Serpone, Is the band gap of pristine TiO_2 narrowed by anion-and cation-doping of titanium dioxide in second-generation photocatalysts? J. Phys. Chem. B 110 (2006) 24287–24293.
[10] X. Chen, S. Shen, L. Guo, S.S. Mao, Semiconductor-based photocatalytic hydrogen generation, Chem. Rev. 110 (2010) 6503–6570.
[11] H.-i. Kim, J. Kim, W. Kim, W. Choi, Enhanced photocatalytic and photoelectrochemical activity in the ternary hybrid of $CdS/TiO_2/WO_3$ through the cascadal electron transfer, J. Phys. Chem. C 115 (2011) 9797–9805.
[12] G. Li, V. Shrotriya, J. Huang, Y. Yao, T. Moriarty, K. Emery, Y. Yang, High-efficiency solution processable polymer photovoltaic cells by self-organization of polymer blends, Nat. Mater. 4 (2005) 864–868.
[13] R. Friend, R. Gymer, A. Holmes, J. Burroughes, R. Marks, C. Taliani, D. Bradley, D. Dos Santos, J. Bredas, M. Lögdlund, Electroluminescence in conjugated polymers, Nature 397 (1999) 121–128.
[14] G. Li, R. Zhu, Y. Yang, Polymer solar cells, Nat. Photonics 6 (2012) 153–161.
[15] F.C. Krebs, Polymer solar cell modules prepared using roll-to-roll methods: knife-over-edge coating: slot-die coating and screen printing, Sol. Energy Mater. Sol. Cells 93 (2009) 465–475.
[16] C.J. Brabec, N.S. Sariciftci, J.C. Hummelen, Plastic solar cells, Adv. Funct. Mater. 11 (2001) 15–26.
[17] J. Janata, M. Josowicz, Conducting polymers in electronic chemical sensors, Nat. Mater. 2 (2003) 19–24.
[18] C. Janaky, N.R. de Tacconi, W. Chanmanee, K. Rajeshwar, Bringing conjugated polymers and oxide nanoarchitectures into intimate contact: light-induced electrodeposition of polypyrrole and polyaniline on nanoporous WO_3 or TiO_2 nanotube array, J. Phys. Chem. C 116 (2012) 19145–19155.
[19] R.J. Nussbaumer, W.R. Caseri, P. Smith, T. Tervoort, Polymer-TiO_2 nanocomposites: a route towards visually transparent broadband UV filters and high refractive index materials, Macromol. Mater. Eng. 288 (2003) 44–49.
[20] W. Feng, E. Sun, A. Fujii, H. Wu, K. Niihara, K. Yoshino, Synthesis and characterization of photoconducting polyaniline-TiO_2 nanocomposite bull, Chem. Soc. Jpn. 73 (2000) 2627–2633.
[21] X.C. Li, J.S. Sun, G.H. He, G.L. Jiang, Y. Tan, B. Xue, Macroporous polypyrrole-TiO_2 composites with improved photoactivity and electrochemical sensitivity, J. Colloid Interface Sci. 411 (2013) 34–40.
[22] J.B. Zhu, X. Zhao, M.L. Xiao, L. Liang, C.P. Liu, J.H. Liao, W. Xing, The construction of nitrogen-doped graphitized carbon-TiO_2 composite to improve the electrocatalyst for methanol oxidation, Carbon 72 (2014) 114–124.
[23] J.J. Li, J.T. Feng, W. Yan, Excellent adsorption and desorption characteristics of polypyrrole/TiO_2 composite for Methylene Blue, Appl. Surf. Sci. 279 (2013) 400–408.
[24] F. Deng, L.J. Min, X.B. Luo, S.L. Wu, S.L. Luo, Visible-light photocatalytic degradation performances and thermal stability due to the synergetic effect of TiO_2 with conductive copolymers of polyaniline and polypyrrole, Nanoscale 5 (2013) 8703–8710.
[25] H. Ullah, K. Ayub, Z. Ullah, M. Hanif, R. Nawaz, A.A. Shah, S. Bilal, Theoretical insight of polypyrrole ammonia gas sensor, Synth. Met. 172 (2013) 14–20.
[26] H. Ullah, A.A. Shah, S. Bilal, K. Ayub, Doping and dedoping processes of polypyrrole: DFT study with hybrid functionals, J. Phys Chem. C 118 (2014) 17819–17830.
[27] S. Bibi, H. Ullah, S.M. Ahmad, A.-u.-H. A. Shah, S. Bilal, A.A. Tahir, K. Ayub, Molecular and electronic structure elucidation of polypyrrole gas sensors, J. Phys Chem. C (2015).
[28] H. Ullah, A.A. Shah, K. Ayub, S. Bilal, Density functional theory study of poly (o-Phenylenediamine) oligomers, J. Phys Chem. C 117 (2013) 4069–4078.
[29] H. Ullah, A.A. Shah, S. Bilal, K. Ayub, DFT study of polyaniline NH3 CO_2, and CO gas sensors: comparison with recent experimental data, J. Phys Chem. C 117 (2013) 23701–23711.
[30] M.J.T. Frisch, G.W. Schlegel, H.B. Scuseria, G.E. Robb, M.A. Cheeseman, J.R. Scalmani, G. Barone, V. Mennucci, B. Petersson, G.A. Gaussian 09, Revision C. 01; Gaussian, Inc.: Wallinford, CT, 2009., Gaussian 09.
[31] A. R. Allouche, Gabedit, http://gabedit.sourceforge.net (2011).
[32] N.M. O'boyle, A.L. Tenderholt, K.M. Langner, Cclib: a library for package-independent computational chemistry algorithms, J. Comp Chem 29 (2008) 839–845.
[33] R. Dennington, T. Keith, and J. G. Millam, Version 5.0. 8 Semichem Inc., Shawnee Mission KS (2008).
[34] J.G. Brandenburg, M. Alessio, B. Civalleri, M.F. Peintinger, T. Bredow, S. Grimme, Geometrical correction for the inter-and intramolecular basis set superposition error in periodic density functional theory calculations, J. Phys. Chem. A 117 (2013) 9282–9292.
[35] H. Kruse, L. Goerigk, S. Grimme, Why the standard B3LYP/6-31G* model chemistry should not be used in DFT calculations of molecular thermochemistry: understanding and correcting the problem, J. Org. Chem. 77 (2012) 10824–10834.
[36] A.M. Asaduzzaman, G. Schreckenbach, Computational studies of the interactions of I- and I3- with TiO_2 clusters: implications for dye-sensitized solar cells, Theor. Chem. Acc. 129 (2011) 199–208.
[37] G.A. Jeffrey, An Introduction to Hydrogen Bonding, vol 12, Oxford university press, New York, 1997.
[38] C. Fonseca Guerra, J.W. Handgraaf, E.J. Baerends, F.M. Bickelhaupt, Voronoi deformation density (VDD) charges: assessment of the Mulliken Bader, Hirshfeld, Weinhold, and VDD methods for charge analysis, J. Comput. Chem. 25 (2004) 189–210.
[39] F. Martin, H. Zipse, Charge distribution in the water molecule—a comparison of methods, J. Comput. Chem. 26 (2005) 97–105.
[40] D.O. Scanlon, C.W. Dunnill, J. Buckeridge, S.A. Shevlin, A.J. Logsdail, S.M. Woodley, C.R.A. Catlow, M.J. Powell, R.G. Palgrave, I.P. Parkin, Band alignment of rutile and anatase TiO2, Nat Mater 12 (2013) 798–801.
[41] N. Martsinovich, D.R. Jones, A. Troisi, Electronic structure of TiO_2 surfaces and effect of molecular adsorbates using different DFT implementations, J. Phys Chem. C 114 (2010) 22659–22670.

Biographies

Habib Ullah received M.Sc degree in Physical Chemistry from Hazara University, Mansehra in 2010 and M.Phil from the Institute of Chemical Sciences, University of Peshawar, Pakistan in 2014. Currently, he is doing Ph.D under the supervision of Dr. Asif and Prof. Tapas, in Renewable Energy, at College of Engineering, Mathematics and Physical Science (CEMPS), University of Exeter, UK. His research involves, Design of novel Materials i.e., conjugated organic polymers (graphene), inorganic metal oxides, perovskites and their composites, for sensors, solar cells, rechargeable batteries, light-emitting diodes, and corrosion inhibition applications.

Asif A. Tahir graduated from the Department of Inorganic Chemistry at Quaid-i-Azam University, Pakistan, in 2009. He worked as a research associate at Loughborough University for three years and then moved to the University of Liverpool before joining the College of Engineering, Mathematics and Physical Sciences (CEMPS) at the University of Exeter as a Lecturer in Renewable Energy. He specializes in the fabrication of nanomaterials using state-of-the-art techniques for solar energy conversion and photocatalysis. His research focus includes the design, synthesis, and characterization of new materials using soft chemistry approaches and the optimization of nanomaterials for high performance.

Tapas K. Mallick received the Ph.D. degree from the University of Ulster, Coleraine, UK, in 2003. From 2007 to 2012, he was a Lecturer with Heriot- Watt University, UK. He is currently a Professor with the Renewable Energy and Chair in Clean Technologies with the Environment and Sustainability Institute, University of Exeter, Penryn, UK. His research interests include renewable energies, concentrating photovoltaics, building integrated photovoltaics, integration of renewables, modelling and biomimicing of solar energy

Please cite this article in press as: H. Ullah, et al., Polypyrrole/TiO_2 composites for the application of photocatalysis, Sens. Actuators B: Chem. (2016), http://dx.doi.org/10.1016/j.snb.2016.10.019